Monodisperse water-soluble magnetite nanoparticles prepared by polyol process for high-performance magnetic resonance imaging†

Jiaqi Wan,[a] Wei Cai,*[a] Xiangxi Meng[b] and Enzhong Liu[b]

Received (in Cambridge, UK) 20th August 2007, Accepted 13th September 2007
First published as an Advance Article on the web 4th October 2007
DOI: 10.1039/b712795b

A new class of monodisperse water-soluble magnetite nanoparticles was prepared by a simple and inexpensive method based on a polyol process, and their potential as MRI contrast agents was investigated.

Magnetite (Fe_3O_4) nanoparticles are currently one of the most promising materials for numerous biomedical applications such as magnetic separation, drug delivery, cancer hyperthermia, and magnetic resonance imaging (MRI).[1–7] In this respect, magnetite nanoparticles must be monodisperse, highly crystalline, and water-soluble to provide reproducible quality, high magnetization values and good biocompatibility under biological conditions. Currently, the vast majority of magnetite nanoparticles used in biomedicine are prepared by the conventional coprecipitation method based on the coprecipitation of iron salts in alkaline aqueous solutions.[8–10] However, some physical characteristics of the nanoparticles, such as broad size distribution, poor crystallinity, low value of saturation magnetization, and aggregation, still need to be improved.[11,12] Recently, high-quality monodisperse iron oxide nanoparticles with high crystallinity and narrow size distribution have been prepared by a high-temperature organic phase decomposition method.[13–17] However, the produced magnetite nanocrystals are only soluble in nonpolar solvents due to the capped hydrophobic surfactant ligand, which limits their applications in the biomedical field unless a complicated surface modification is employed.[18–21] In order to successfully address these issues in the synthesis of iron oxide nanoparticles, there is a need to develop a new synthetic technique for fabrication of water-soluble magnetite nanoparticles that are suitable for biomedical applications.[22,23] In the present paper, intrinsically water-soluble magnetite nanoparticles with sizes smaller than 10 nm, narrow size distribution, and high magnetization were prepared by a polyol process, a term which often refers to the formation of fine particles by heating salts in polyalcohols.[24,25] Unlike particles synthesized by an organic phase decomposition method, these novel magnetite nanoparticles are intrinsically stabilized with a layer of hydrophilic polyol molecules, and exhibit long-term colloidal stability in aqueous media without any surface modification. MRI measurements indicate the nanoparticles have the desired relaxivity values for MR signal enhancement. *In vitro* experiments show that the nanoparticles are biocompatible and are taken up readily by glioma cells, suggesting that these magnetite nanoparticles have potential as MRI contrast agents for biomedical research and clinical diagnosis.

The synthesis of the magnetite nanoparticles was carried out by reacting an iron precursor, iron(III) acetylacetonate ($Fe(acac)_3$), in the polyol medium triethylene glycol (TREG) at elevated temperature without any surfactants.[26,27] The polyol TREG in this reaction plays a triple role as high-boiling solvent, reducing agent, and stabilizer to efficiently control the particle growth and prevent interparticle aggregation. The details of the synthetic procedures are given in ESI.†

Fig. 1 shows representative TEM images of the magnetite nanoparticles. It is clear that the synthesized nanoparticles are uniform in size and non-aggregated. The particle size is found to be 8 ± 1.1 nm which is in the superparamagnetic size range. HRTEM analysis demonstrated that as-synthesized nanoparticles are single crystals. The lattice spacing between two adjacent planes is 0.25 nm, corresponding to the distance between two (311) planes in spinel-structured Fe_3O_4. Selected area electron diffraction (SAED) and X-ray diffraction (XRD) analysis further proved that the nanoparticles are highly crystalline magnetite nanoparticles (see ESI Fig. S1†). Magnetic measurements confirmed that the particles are superparamagnetic at room temperature. The saturation magnetization of the sample is 80 emu g^{-1} at room temperature (see ESI Fig. S2†), which is stronger than that of magnetite nanoparticles obtained by the aqueous phase methods. The relatively higher reaction temperature (278 °C) of this system favors materials with a higher crystallinity and, consequently, higher magnetization.

FTIR spectra and TGA analysis of the nanoparticles both revealed the existence of TREG as stabilizer on the surface of Fe_3O_4 (see ESI Figs. S3, S4†). X-ray photoelectron spectra (XPS) of the particles (see ESI Fig. S5†) further showed that the

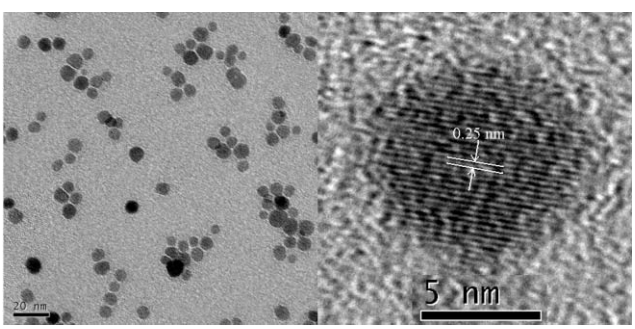

Fig. 1 Representative TEM image (left) and HRTEM image (right) of as-synthesized magnetite nanoparticles.

[a]*School of Material Science and Engineering, Harbin Institute of Technology, Harbin, Heilongjiang 150001, China. E-mail: wjiaq@hit.edu.cn; Fax: 86-451-86415083; Tel: 86-451-86418649*
[b]*Department of Neurosurgery, The First Affiliated Hospital of Harbin Medical University, Harbin, Heilongjiang 150001, China*
† Electronic supplementary information (ESI) available: Experimental details and Figs. S1–S6. See DOI: 10.1039/b712795b

nanoparticles are rich in surface hydroxyl groups although the exact reaction mechanism is not yet clear. However, this fact suggests the adsorption of TREG on magnetite nanoparticles might be *via* hydrogen bonding interactions between TREG and both the surface oxygen and hydroxyl groups on the Fe_3O_4 surface during the synthesis step.

The obtained magnetite nanoparticles can easily be dispersed in aqueous media without any further surface modification. Dynamic light scattering (DLS) measurements revealed that the nanoparticles are highly monodisperse in aqueous media. The hydrodynamic diameter of the particles in water is found to increase to 16.5 $\pm$ 3.5 nm due to the presence of the associated and hydrated TREG layer (Fig. 2a). The nanoparticles can also form a stable dispersion in PBS buffer solution which has the same pH value and ionic strength as physiological conditions. This colloid remains stable for several months without noticeable pecipitation, as shown in Fig. 2b. The non-aggregated nature of the particles in physiological buffer was confirmed by TEM analysis (Fig. 2c).

To investigate the MR signal enhancement effects, the aqueous solutions of as-prepared magnetite nanoparticles at different Fe concentrations (determined by ICP-AES) were measured on a clinical 1.5 T MRI scanner. As shown in Fig. 3a, both T_1 and T_2 weighted images change drastically in signal intensity with an increasing amount of magnetite nanoparticles, indicating that as-synthesized magnetite nanoparticles generated MR contrast on both longitudinal (T_1) and transverse (T_2) proton relaxation times-weighted sequences. Fig. 3b shows the relaxation rates $1/T_1$ and $1/T_2$ as a function of the iron concentration for the magnetite nanoparticles. It was found that the relaxation rates varied linearly with the iron concentration, according to the following equation:

$$1/T_{1,2} = 1/T^0_{1,2} + r_{1,2}\cdot[\mathrm{Fe}] \quad (1)$$

where $1/T_{1,2}$ is the observed relaxation rate in the presence of magnetite nanoparticles, $1/T^0_{1,2}$ is the relaxation rate of pure water, [Fe] is the concentration of magnetite nanoparticles, and r_1 and r_2 are the longitudinal and transverse relaxivities, which represent the efficiency of the magnetite nanoparticles as a contrast agent shortens the proton relaxation times. The r_1 and r_2 relaxivities of as-synthesized magnetite nanoparticles are found to be 14.14 Fe mM^{-1} s^{-1} and 82.68 Fe mM^{-1} s^{-1}, respectively. Such values for r_1 and r_2 suggest that

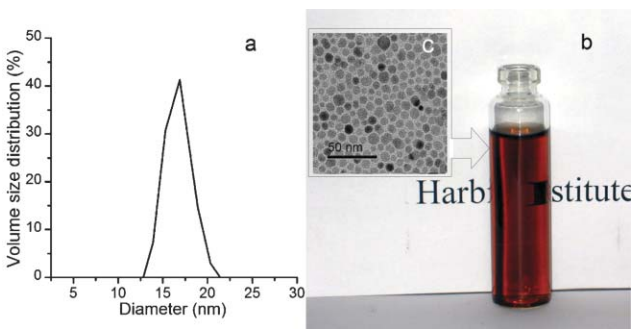

Fig. 2 (a) Dynamic light scattering (DLS) of the aqueous dispersion of as-synthesized magnetite nanoparticles; (b) photograph of PBS buffer suspension of the magnetite nanoparticles; (c) TEM image of the PBS buffer suspension of the magnetite nanoparticles.

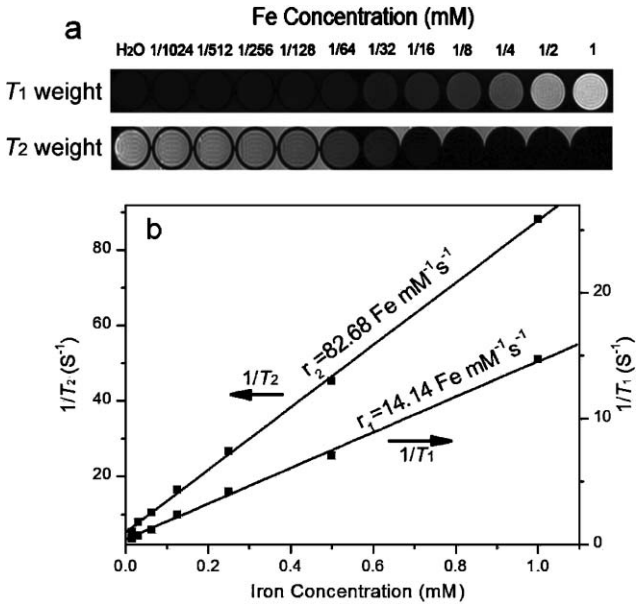

Fig. 3 (a) T_1 weight MR images and T_2 weight MR images of aqueous solutions of as-synthesized magnetite nanoparticles at different Fe concentrations; (b) T_1 and T_2 relaxation rates ($1/T_1$, $1/T_2$) plotted against the Fe concentration for the magnetite nanoparticles aqueous solutions.

as-synthesized magnetite nanoparticles can act as both T_1 and T_2 contrast agents taking into account their ultra-small size, but seem to be more favorable as T_2 contrast agents due to their much larger r_2 value.

Cellular uptake of the magnetite nanoparticles was investigated in the rat C6 glioma cell line. Fig. 4A shows the optical micrographs of Prussian blue stained C6 cells after 4 h incubation with 100 Fe μg mL^{-1} magnetite nanoparticles. It can be seen that most of the C6 glioma cells (99.6%) incubated with magnetite nanoparticles are stained in blue, whereas no blue spots were observed in the cytoplasm of the control normal neural cells treated with magnetite nanoparticles under the same conditions (Fig. 4B). These results indicate a high uptake of the magnetite nanoparticles in C6 glioma cell lines instead of normal neural cells. The strong interaction between the magnetite nanoparticles and C6 glioma cells might arise from the unusual metabolism activity of cancer cells as well as the ultrasmall size effect of the particle.[28] The MR imaging of the cells was subsequently performed on a clinical 1.5 T MRI scanner by suspending the cells in agarose gel. In T_2 weighted images, a significant darkening of T_2 weighted

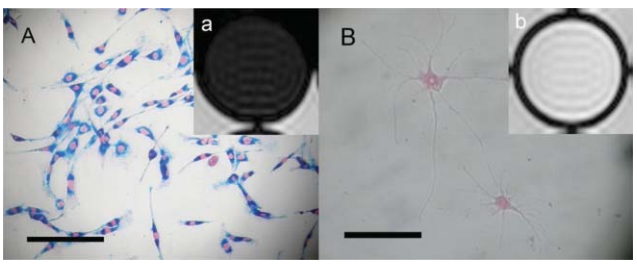

Fig. 4 Prussian blue staining images of (A) rat C6 glioma cells and (B) neural cells incubated with as-synthesized magnetite nanoparticles for 4 h. Insets are the corresponding T_2 weight images. Bars = 200 μm.

signals is seen for the C6 cells (Fig. 4a), whereas no MR contrast is observed from the control normal neural cells (Fig. 4b). The MRI measurements are consistent with the results obtained through Prussian blue staining. This phenomenon indicates that our magnetite nanoparticles have great potential as a biomarker for cancer cells imaging *in vivo* given their small size and unique hydrophilic surface nature.[29] The cytotoxicity of as-prepared magnetite nanoparticles on C6 and normal neural cells was also evaluated by MTT assay. The results indicate that the viability of the cells is not affected by the presence of magnetite nanoparticles even up to 200 Fe mg L^{-1}, suggesting that our magnetite nanoparticles are highly biocompatible and safe for further *in vivo* use (see ESI Fig. S6†). An *in vivo* pharmacokinetics study of the circulation and biodistribution of these novel magnetite nanoparticles in animal models is currently under way.

In summary, a new class of magnetite nanoparticles has been synthesized by a simple and effective route based on high-temperature decomposition of $Fe(acac)_3$ in TREG. The nanoparticles are uniform in size, highly crystalline, and superparamagnetic at room temperature. The unique hydrophilic surface structures of the particles lead to the particles being stable not only in aqueous solution at neutral pH but also in physiological buffer. *In vitro* experiments have shown that these magnetite nanoparticles have an excellent MRI enhancement effect, unusual cancer cellular affinity and good biocompatibility. Therefore, these novel magnetite nanoparticles should have great potential as high-performance MRI contrast agents for cell or molecular imaging and diagnostic applications.

The authors thank Prof. Hui Li of Yansan University for her help with the TEM study. This work is supported by the National Natural Science Foundation of China (No. 50531020).

Notes and references

1 C. C. Berry1 and A. S. G. Curtis, *J. Phys. D: Appl. Phys.*, 2003, **36**, R198.
2 Q. A. Pankhurst, J. Connolly, S. K. Jones and J. Dobson, *J. Phys. D: Appl. Phys.*, 2003, **36**, R167.
3 S. Mornet, S. Vasseur, F. Grasset and E. Duguet, *J. Mater. Chem.*, 2004, **14**, 2161.
4 H. Gu, K. Xu, C. Xu and B. Xu, *Chem. Commun.*, 2006, 941.
5 F. Hu, L. Wei, Z. Zhou, Y. Ran, Z. Li and M. Gao, *Adv. Mater.*, 2006, **18**, 2553.
6 J.-H. Lee, Y.-w. Jun, S.-I. Yeon, J.-S. Shin and J. Cheon, *Angew. Chem., Int. Ed.*, 2006, **45**, 8160.
7 S. A. Corr, A. O'Byrne, Y. K. Gun'ko, S. Ghosh, D. F. Brougham, S. Mitchell, Y. Volkov and A. Prina-Mellod, *Chem. Commun.*, 2006, 4474.
8 R. Massart, *IEEE Trans. Magn.*, 1981, **17**, 1247.
9 R. Weissleder, A. A. Bogdanov, E. A. Neuwelt and M. Papisov, *Adv. Drug Delivery Rev.*, 1995, **16**, 321.
10 S. Mornet, J. Portier and E. Duguet, *J. Magn. Magn. Mater.*, 2005, **293**, 127.
11 E. Taboada, E. Rodríguez, A. Roig, J. Oró, A. Roch and R. N. Muller, *Langmuir*, 2007, **23**, 4583.
12 J. Qin, S. Laurent, Y. S. Jo, A. Roch, M. Mikhaylova, Z. M. Bhujwalla, R. N. Muller and M. Muhammed, *Adv. Mater.*, 2007, **19**, 1874.
13 J. Rockenberger, E. C. Scher and A. P. Alivisatos, *J. Am. Chem. Soc.*, 1999, **121**, 11595.
14 T. Hyeon, S. S. Lee, J. Park, Y. Chung and H. B. Na, *J. Am. Chem. Soc.*, 2001, **123**, 12798.
15 S. Sun, H. Zeng, D. B. Robinson, S. Raoux, P. M. Rice, S. X. Wang and G. X. Li, *J. Am. Chem. Soc.*, 2004, **126**, 273.
16 W. W. Yu, J. C. Falkner, C. T. Yavuz and V. L. Colvin, *Chem. Commun.*, 2004, 2306.
17 N. R. Jana, Y. Chen and X. Peng, *Chem. Mater.*, 2004, **16**, 3931.
18 M. Lattuada and T. A. Hatton, *Langmuir*, 2007, **23**, 2158.
19 Y.-M. Huh, Y.-W. Jun, H.-T. Song, S. Kim, J.-S. Choi, J.-H. Lee, S. Yoon, K.-S. Kim, J.-S. Shin, J.-S. Suh and J. Cheon, *J. Am. Chem. Soc.*, 2005, **127**, 12387.
20 C. Xu, K. Xu, H. Gu, R. Zheng, H. Liu, X. Zhang, Z. Guo and B. Xu, *J. Am. Chem. Soc.*, 2004, **126**, 9938.
21 W. W. Yu, E. Chang, C. M. Sayes, R. Drezek and V. L. Colvin, *Nanotechnology*, 2006, **17**, 4483.
22 (*a*) Z. Li, H. Chen, H. Bao and M. Gao, *Chem. Mater.*, 2004, **16**, 1391; (*b*) Z. Li, L. Wei, M. Gao and H. Lei, *Adv. Mater.*, 2005, **17**, 1001.
23 N. Pinna, S. Grancharov, P. Beato, P. Bonville, M. Antonietti and M. Niederberger, *Chem. Mater.*, 2005, **17**, 3044.
24 F. Fievet, J. P. Lagier, B. Blin, B. Beaudoin and M. Figlarz, *Solid State Ionics*, 1989, **32–33**, 198.
25 C. Feldmann and G.-O. Jungk, *Angew. Chem., Int. Ed.*, 2001, **40**, 359.
26 W. Cai and J. Wan, *J. Colloid Interface Sci.*, 2007, **305**, 366.
27 J. Wan, W. Cai, J. Feng, X. Meng and E. Liu, *J. Mater. Chem.*, 2007, **17**, 1188.
28 C. Zimmer, R. Weissleder, K. Poss, A. Bogdanova, S. C. Wright and W. S. Enochs, *Radiology*, 1995, **197**, 533.
29 C. Corot, P. Robert, J.-M. Idée and M. Port, *Adv. Drug Delivery Rev.*, 2006, **58**, 1471.

